Monatshefte für Chemie - Chemical Monthly
https://doi.org/10.1007/s00706-018-2237-4

ORIGINAL PAPER

Mimic catechins to develop selective MMP-2 inhibitors

Antonella Di Pizio[1] · Mariangela Agamennone[2] · Antonio Laghezza[3] · Fulvio Loiodice[3] · Paolo Tortorella[3]

Received: 25 March 2018 / Accepted: 19 May 2018

Abstract
Matrix metalloproteinase 2 (MMP-2) is a well-known anticancer target belonging to the MMP family. Because of the bilateral role of MMPs in cancer, developing highly selective MMP-2 inhibitors is a current challenge. In this paper, we investigated the binding modes of green tea polyphenols epigallocatechin gallate and epicatechin into the active site of the MMP-2 enzyme. The structure-based analysis allowed the optimization of these hits and hence led to a better lead candidate. Moreover, using a pharmacophore model, we screened FooDB compounds and selected food components as potential MMP-2 inhibitors. The search for food-derived compounds that target this enzyme may represent a strategy to identify new lead molecules with improved safety profiles and provide indications about possible functional foods.

Graphical abstract

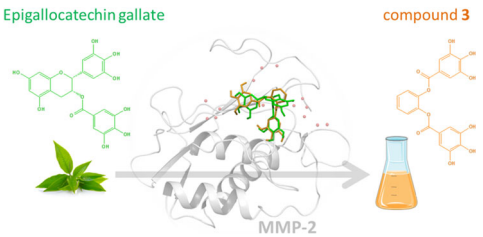

Keywords Enzymes · Ligands · Molecular modelling · Flavonoids · MMP inhibitors · Anticancer drugs

Introduction

Although diet–cancer relationships are complex and of difficult characterization, there is a scientific evidence of the role assumed by particular foods in cancer prevention [1, 2]. Interestingly, some food-derived compounds are even under evaluation for cancer treatment. For instance, curcumin is a component of turmeric (*Curcuma longa*), used as a folk medicine in India for 4000 years, potentially applicable in cancer treatment owing to its capability of killing carcinogenic cells without harming adjacent healthy cells [3]. Substances with physiological benefits other than nutrition usually have fewer side effects compared to pharmaceuticals and would be an interesting direction for the discovery and development of new anticancer drugs [4–6]. Conventional anticancer drug discovery focused for a long time on cytotoxic agents. Nowadays, it is still a challenge to develop new, effective, and affordable anticancer drugs acting by mechanisms that may not result in significant toxicity.

Metastasis production, i.e., the spread of the tumor from one organ or part of the body to another, remains the major driver of mortality in patients with cancer. The process of tumor cell translocation requires cellular movement as well as the remodeling of the extracellular matrix (ECM).

✉ Antonella Di Pizio
adipizio@mail.huji.ac.il

[1] Institute of Biochemistry, Food Science and Nutrition, The Robert H. Smith Faculty of Agriculture, Food and Environment, The Hebrew University, Rehovot, Israel

[2] Dipartimento di Farmacia, Università "G. d'Annunzio", Chieti-Pescara, Chieti, Italy

[3] Dipartimento di Farmacia-Scienze del Farmaco, Università degli Studi "A. Moro" di Bari, Bari, Italy

Published online: 08 June 2018

Matrix metalloproteinases (MMPs) are zinc-dependent ECM-degrading-endopeptidases. 23 MMPs have been identified in humans, and, despite their high structural similarity, no functional redundancy is shared between them [7]. Each MMP influences ECM properties differently, and consequently, enzyme selectivity is essential to develop MMP inhibitors, especially for anticancer therapy. Indeed, MMP-2 and MMP-9 essentially contribute to the invasion and dissemination of tumor cells [8], but several MMPs showed protective effects in cancer [9], with MMP-8 as a recognized anti-target [10, 11].

Commonly, synthetic MMP inhibitors (MMPIs) consist of a metal coordinating function, called zinc-binding group (ZBG), as it binds to the catalytic zinc, and moieties that reach into surrounding binding pockets. The binding to the zinc ion ensures the potency, while the interaction with the pockets modulates the selectivity of the inhibitor. The hydroxamate function is one of the most used ZBGs for the development of potent MMPIs [12]. However, it is characterized by a poor pharmacokinetic profile and by toxic effects in long-term treatments [13]. To overcome the problems of selectivity and/or toxicity, two approaches have been followed to synthesize MMPIs: the use of alternative ZBGs [14–16] and the development of novel non-competitive inhibitors not interacting with the catalytic zinc (also classified as the third generation MMPIs) [17–19].

Intriguingly, several natural compounds have shown promising inhibition of MMP-2, including curcumin from *Curcuma longa*, polyphenols from *Camellia sinensis*, ageladine A from the marine sponge *Agelas nakamurai*, fucoidan extracts from seaweeds *Claisiphon novaecaledoniae*, and methanolic extracts from marine red algae *Cavalina pilulifera* [20–23]. This opens the possibility of using non-toxic natural compounds as starting points for a drug design project. Here, the putative binding modes of (–)-epicatechin (**1**, EC) and (–)-epigallocatechin gallate (**2**, EGCG), polyphenols from *Camellia sinensis*, have been investigated. This work provides insights for the optimization of catechins as selective MMP-2 inhibitors and suggests the molecular features that lead to enzyme inactivation. Moreover, we generated a structure-based pharmacophore model that was used to virtually screen food-derived compounds (collected in the freely available FooDB database, http://foodb.ca/). Highly scored molecules were selected as potential MMP-2 inhibitors.

Results and discussion

Green tea polyphenol (−)-epigallocatechin gallate (**2**) was found to inhibit the growth of malignant cells via modulation of MMP-2 [24]. While EGCG (**2**) inhibits markedly MMP-2 activities, epicatechin (**1**) did not show noticeable inhibition of the enzyme activity [25]. EGCG and analogs have been previously tested on MMP-9, and the pyrogallol hydroxyl groups were shown to be essential for MMP-9 inhibition [26]. Interestingly, it has been found that the gallate itself inhibits MMPs and is more selective on MMP-2 than on MMP-8 [15]. To understand the molecular features that are responsible for the MMP-2 binding and inactivation, we performed a structure-based analysis of EC (**1**) and EGCG (**2**) into the MMP-2 enzyme, which then led to the design of compound **3**. EC (**1**) and EGCG (**2**) were purchased from Aldrich Chemicals (Milan, Italy); compound **3** was obtained via condensation of tribenzyloxybenzoic acid with resorcinol and debenzylation of the resulting ester through catalytic hydrogenation (Scheme 1).

Even though EGCG is active in preventing also the proMMP-2 activities [25], we focused our analysis on the active form of MMP-2. Particularly, EC (**1**), EGCG (**2**), and compound **3** were submitted to enzyme inhibition assays for MMP-2, but also for MMP-9 and MMP-8, which, as mentioned above, are considered target and anti-target, respectively, for cancer therapy (Table 1).

Binding modes of EGCG and EC into MMP-2 enzyme

Previous attempts were done to identify the binding mode of the green tea polyphenols into the MMP-2 enzyme [25]. Docking studies by Chowdhury et al. suggested that EC and EGCG H-bond with Glu202 side chain through the catechol and the pyrogallol, respectively; instead, the benzodihydropyran of the two ligands is oriented differently, forming an H-bond with the Pro221 main chain in the case of EC and with the backbone of Leu197 and His201 residues in the case of EGCG.

Recently, the MMP-8 enzyme was crystallized in complex with *N*-(3,4-dihydroxyphenyl)-4-diphenylsulfonamide (Fig. 1), and, using the X-ray structure (PDB ID: 5H8X), the binding modes of several catechol-containing inhibitors into MMP-2, -8, and -9 have been investigated. This analysis revealed a pivotal role of water molecules in mediating the ligand–protein interaction [27]. As shown in Fig. 1, three clusters of water molecules were observed around the catalytic site.

The work from Tauro et al. [27] provides valuable tools to further analyze the binding mode of polyphenolic compounds into MMPs. Particularly, we characterized the binding conformation of EC and EGCG into the MMP-2, MMP-8, and MMP-9 enzymes by superimposing EC and EGCG to the ligand co-crystallized with MMP-8 (PDB ID: 5H8X). Then, the complexes of EC and EGCG with the MMP-2, -8, and -9 were generated and minimized.

In the MMP-2 enzyme, the catechol of EC establishes an H-bond with Glu202 side chain (Fig. 2), as previously

Scheme 1

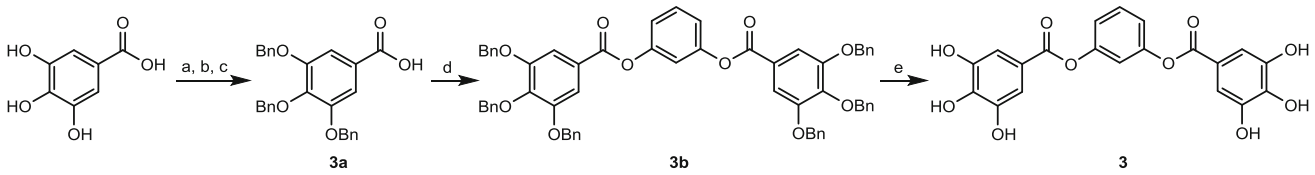

Table 1 MMP activity values expressed as IC_{50}

Compounds	Structure	IC_{50} /μM		
		MMP-2	MMP-8	MMP-9
1 (EC)*	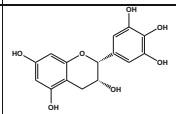	63±4%	45±7%	41±5%
2 (EGCG)	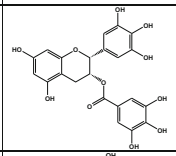	102±15	260±40	120±10
3	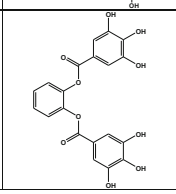	26±5	95±8	20±9

*IC_{50} not available; percentage of inhibition has been measured at 1 mM

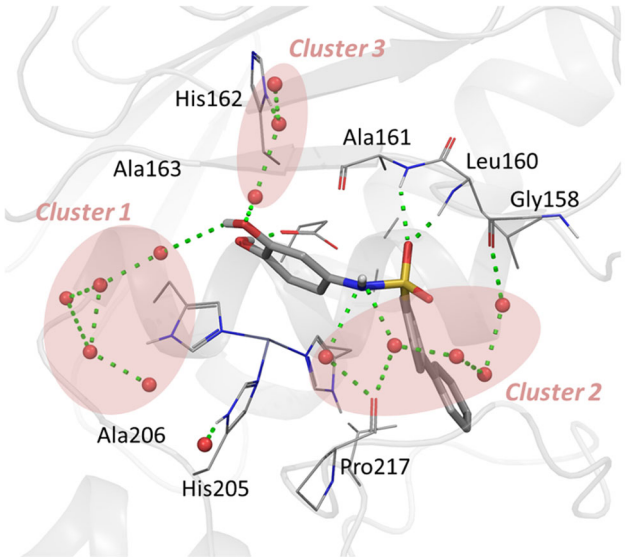

Fig. 1 Three water clusters mediating the ligand-binding interaction in MMP-8 as determined by X-ray (PDB ID: 5H8X). Ligand is represented in CPK sticks, interacting residues as thin sticks, and water molecules as red spheres. H-bonds are shown as green dashed lines

suggested by Chowdhury et al. [25]. Similarly, the pyrogallol and the benzodihydropyran of EGCG form H-bonds with Glu202 and Pro221, respectively. Interestingly, the gallate, present in EGCG but not in EC, enters in the S1′ pocket, providing an explanation for the improved potency of EGCG compared to EC (Fig. 2).

Notably, the benzodihydropyran ring of EC and EGCG occupies the region of water cluster 2, disrupting the water-mediated H-bond network between the ligand and Pro221 CO in the primary specificity loop surrounding the S1′ site (Fig. 3a).

The binding mode of EGCG into MMP-8 and -9 is very similar, but the H-bond formed between the meta OH of the benzodihydropyran ring and Pro221 CO in MMP-2/EGCG is maintained with Pro421 in MMP-9/EGCG (Fig. 3b), but is not observed in MMP-8/EGCG (Fig. 3c). Therefore, we suppose that this H-bond, direct or mediated by water cluster 2, may be relevant for the enzymatic activity. These results support the importance of the specificity loop in the MMP activation. In fact, it was hypothesized that the inhibitory activity of non-zinc-binding inhibitors could derive from the freezing effect that ligands produce on this loop [17, 18, 28].

It is well known that the rearrangement of water molecules strongly affects the binding affinity [29, 30]. The cost of displacing ordered or partially ordered water molecules in the protein active site may favorably contribute to the stability of the ligand–protein complex through hydrophobic interactions and a gain of disorder in the solvent [31]. However, some water molecules, also called “happy waters”, play an important stabilizing effect and their displacement decreases the binding affinity [32, 33].

Hit optimization

As a first attempt to test our models and investigate the role of water cluster 2, we synthesized compound **3**. The benzodihydropyran was replaced with a benzene ring that is connected with two pyrogallol rings through ester linkers. By replacing the bicyclic moiety with a benzene ring, the water-mediated connection between the ligand and the Pro221 in the S1′ loop is restored (Fig. 4). Beyond the difference in cluster 2, compared to EGCG, compound **3**

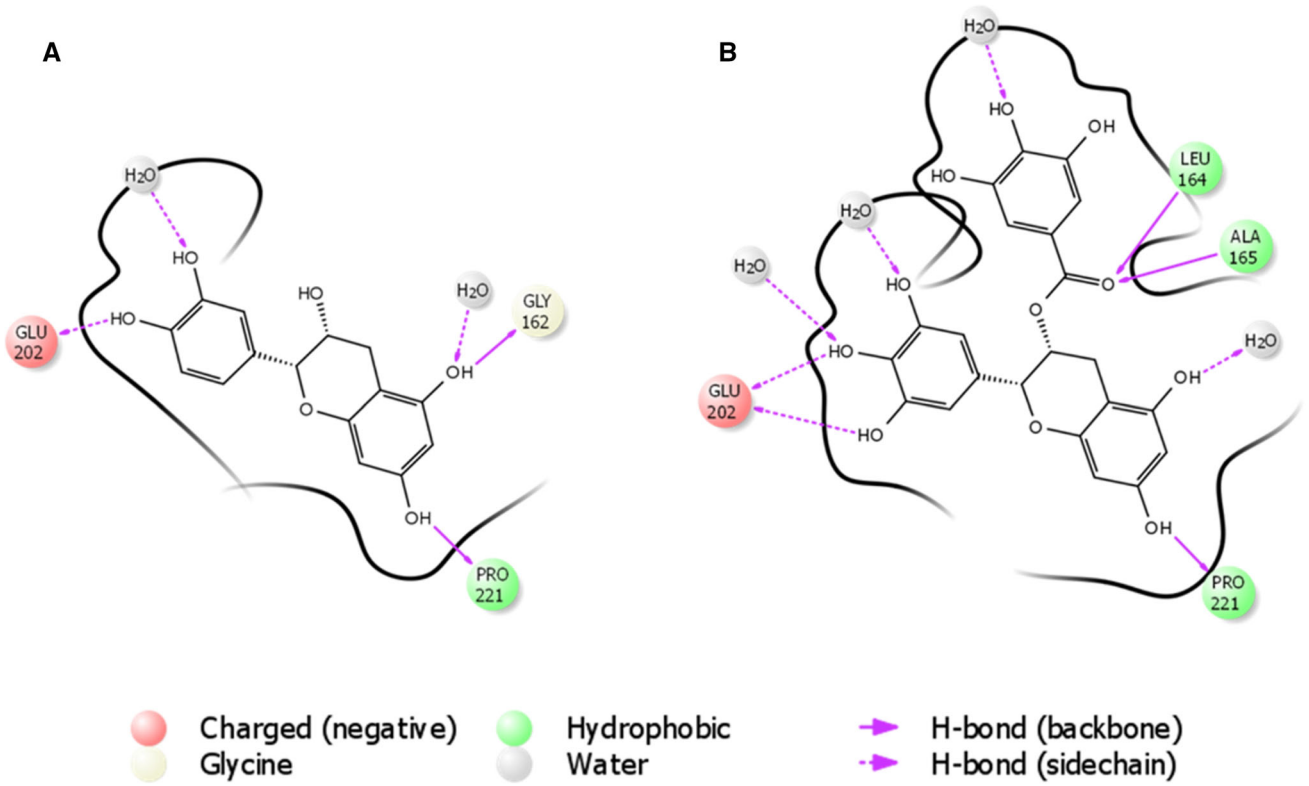

Fig. 2 2D representation of EC and EGCG into the MMP-2 active site. **a** MMP-2/**1** (predicted total energy: − 413 kJ/mol); **b** MMP-2/**2** (predicted total energy: − 561 kJ/mol). The total energy of the minimized complexes is used as an estimation of the binding affinity

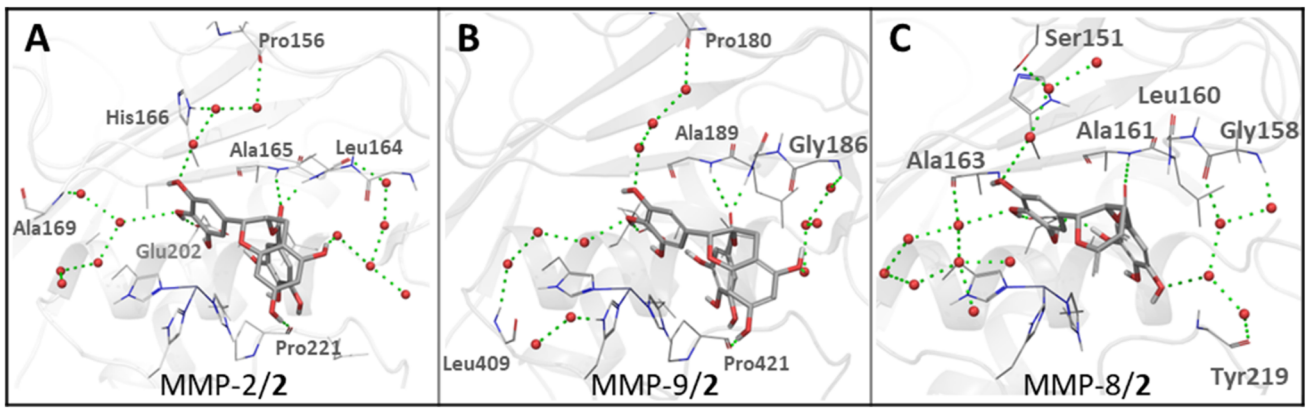

Fig. 3 3D representations of the putative binding modes of EGCG into MMP-2, -9 and -8. **a** MMP-2/**2** (predicted total energy: − 561 kJ/mol); **b** MMP-9/**2** (predicted total energy: − 634 kJ/mol); **c** MMP-8/**2** (predicted total energy: − 526 kJ/mol). The total energy of the minimized complexes is used as an estimation of the binding affinity. Ligands are represented in CPK sticks, interacting residues as thin sticks, and water molecules as red spheres. H-bonds are shown as green dashed lines

orients the gallate moiety in the proximity of the zinc differently: the ortho OH group established the H-bond with Glu202 instead of the meta OH of EGCG. The second gallate moiety enters in the S1′ pocket and establishes hydrophobic interactions with His201 (Fig. 4), with a comparable conformation of the EGCG gallate (Fig. 3a).

The enzyme assays revealed an improved potency of compound **3** towards tested MMPs compared to EGCG, maintaining certain selectivity against MMP-8 (Table 1). The predicted energies of the complexes MMP-2/**3**, MMP-8/**3,** and MMP-9/**3** (− 546, − 472, and − 559 kJ/mol, respectively) are in good correlation with the experimental IC_{50} values. Our results suggest that the benzodihydropyran ring does not establish favorable hydrophobic interactions, and instead, the connection between the ligand and the S1′ loop mediated by water molecules is preferred. This is reasonable considering that the benzodihydropyran ring occupies a solvent-exposed region.

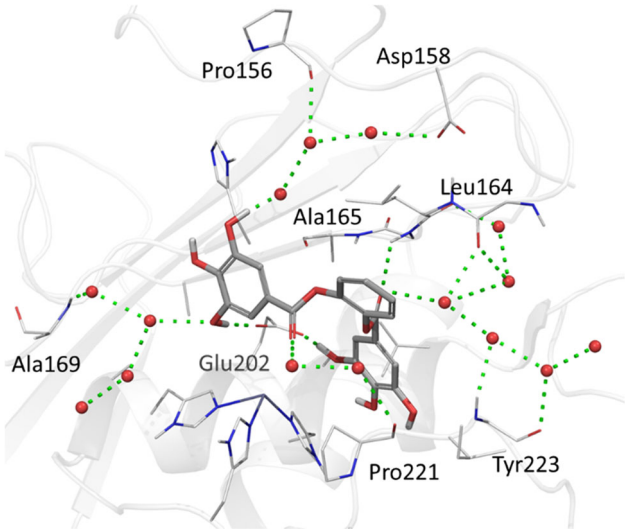

Fig. 4 3D representations of the putative binding mode of compound **3** into MMP-2. Ligand is represented in CPK sticks, interacting residues as thin sticks, and water molecules as red spheres. H-bonds are shown as green dashed lines

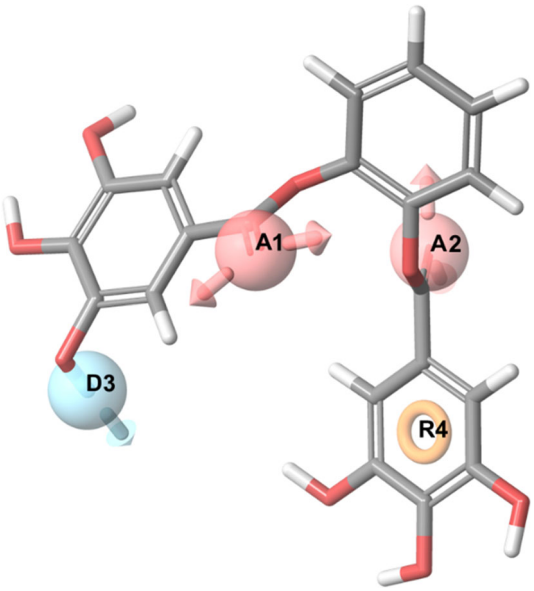

Fig. 5 Pharmacophore model AADR. A1 and A2 represent H-bond acceptors, D3 H-bond donor, and R4 the aromatic ring). Acceptor (red) and donor (cyan) features are shown as spheres and vectors, and aromatic feature as orange ring

Compound **3** can be considered a good candidate for further optimization; simplifying the linker between the two pyrogallol rings, improving the coordination with the zinc ion, and enlarging the gallate residue to the S1′ pocket may indeed lead to increased potency.

Virtual screening of FooDB compounds

The structure-based analysis of compounds **1**-**3** into the MMP-2 enzyme provides insights into the molecular features needed for MMP-2 selective inhibition, which has been summarized in a pharmacophore hypothesis (Fig. 5).

The pharmacophore hypothesis maps the functional groups of compound **3** that are supposed to be essential for MMP-2 inhibition. The acceptor group A1 corresponds to the oxygen that interacts with water cluster 2 and acceptor group A2 to the oxygen H-bonding with Leu164 NH. The donor group D3 accounts for the hydroxyl group H-bonded with Glu202. This feature was identified also by the computational analysis of catechol-containing inhibitors [27], and experimentally in the SAR analysis by Dell'Agli et al. [26]. The aromatic ring that occupies the S1′ site is mapped by the feature R4.

Using the pharmacophore model, FooDB library (∼ 25,000 food constituents—http://foodb.ca/) was virtually screened to predict potential MMP-2 inhibitors and to look for additional scaffolds among food-derived compounds. For the screening, excluded volumes have been added to the pharmacophore model, including all heavy atoms in a range of 5 Å from the ligand. Interestingly, the screening succeeded to retrieve several EGCG derivatives and compounds that are known to affect MMP-2 activity, such as naringenin [34] and butein [35], among the highest ranking molecules. In Table 2, we report molecules that obtained highly ranking scores in the screening and are suggested as novel chemicals to be tested as MMP-2 inhibitors.

Concluding remarks and future perspectives

MMP-2 is considered a relevant drug target for anticancer therapy, and EGCG is an interesting hit molecule to develop MMP-2 inhibitors. We, therefore, investigated the binding mode of EGCG in the active form of MMP-2 to identify the molecular features responsible for enzyme inactivation and design synthetic strategies to improve the potency of MMP-2 inhibitors.

As previously raised [27], our analysis highlights a relevant role of water molecules in the ligand–protein interaction. Indeed, water molecules affect the function of MMP enzymes by taking part in the activation mechanism [36–38]. Happy waters can be involved in drug design, either by conserving their positions and mediating ligand–protein interactions, or by being targets of ligand functional groups. Here, we propose water cluster 2 as an ordered group of molecules that should be conserved to improve the binding affinity. However, several tools were developed and can be applied to extend the analysis of the water molecules in the binding site of MMP-2 [39].

Table 2 FooDB compounds selected with the pharmacophore

Name	Origin	Structure	Fitness value
Xanthoxylol	*Zanthoxylum piperitum*	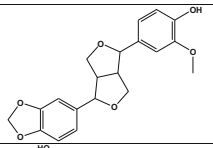	1.89
Mandelonitrile sophoroside	*Perilla frutescens*	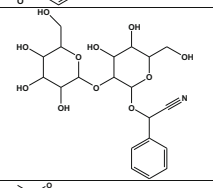	1.85
3'-(6"-Galloylglucosyl)-phloroacetophenone	*Syzygium aromaticum*	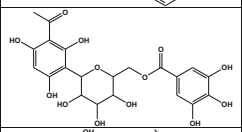	1.8
Carissanol	*Carissa edulis*	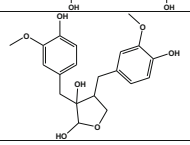	1.74

Fitness values range from zero, lowest score, to 3, highest score

Based on catechin structures, we provide new directions to develop MMP-2 inhibitors: we synthesized a micromolar MMP-2 lead candidate and developed a pharmacophore model used to predict new potential MMP-2 inhibitors among food-derived compounds. Experimental testing of these compounds can reveal new hits for a drug discovery process.

Methods

Computational approaches

EGCG and EC were manually built using the built facility in Maestro; 3D structures and protonation states at pH 7.0 ± 0.5 were generated with LigPrep (Schrödinger, LLC, New York, NY, 2017). Using Phase Shape Screening (Phase, version 5.1, Schrödinger, LLC, New York, NY, 2017), we superimposed compounds **1**–**3** to the binding conformation of *N*-(3,4-dihydroxyphenyl)-4-diphenylsulfonamide in complex with MMP-8, as determined by X-ray (PDB ID: 5H8X), and in complex with MMP-2 and MMP-9, as modelled in Tauro et al. 2016 [27]. Therefore, compounds **1**–**3** in complex with MMP-2, -8, and -9, with explicit waters have been generated and minimized to a derivative convergence of 0.05 kJ/mol Å using the Polak-Ribiere Conjugate Gradient (PRCG) minimization algorithm, the OPLS2005 force field, with MacroModel Embrace Minimization (MacroModel, Schrödinger, LLC, New York, NY, 2017). A shell of 15 Å around the catalytic zinc was set to be free to move, another shell of 5 Å minimized applying a force constant of 200 kJ/mol Å^2, maximum number of steps 15,000. The interaction energy between the receptor and each ligand was calculated with the interaction energy mode implemented in Embrace.

FooDB compounds were prepared with LigPrep and Phase Database. Pharmacophore model AADR was manually built. Using MMP-2/**3** complex, excluded volumes were created on heavy atoms around 5 Å from the ligand, including water molecules. The screening was organized in two different stages. A fast screening was performed using the following settings: rapid sampling, inter-site distance matching tolerance of 1.5 Å, and two out four site points set to be matched, with preference of partial matches involving more sites. 2000 hits returned from the fast screening were submitted to a more accurate screening, with the following settings: thorough sampling, inter-site distance matching tolerance of 1.5 Å, and three out four site points (preferring partial matches involving more sites) set to be matched.

Throughout the text, MMP residues are numbered according the structures deposited in the Protein Data Bank (PDB): 1QIB.pdb for MMP-2 [40], 1GKC.pdb for MMP-9 [41], and 5H8X.pdb for MMP-8 [27].

Chemistry

Mass spectra were recorded on an HP MS 6890-5973 MSD spectrometer, electron impact 70 eV, equipped with an HP ChemStation or with an Agilent LC–MS 1100 Series LC–MSD Trap System VL spectrometer, electrospray ionization (ESI). ^{1}H NMR spectra were recorded using the suitable deuterated solvent on a Varian Mercury 300 NMR Spectrometer. Chemical shifts (δ) are expressed as parts per million (ppm). Flash column chromatography was performed using Geduran silica gel 60 Å (45–63 μm). Chemicals were purchased from Aldrich Chemicals (Milan, Italy) and were used without any further purification.

3,4,5-Tris(benzyloxy)benzoic acid (3a) Gallic acid (1.5 g, 8.83 mmol) was dissolved in 9 cm^3 methanol, conc. 0.45 cm^3 sulfuric acid was added thereto, and the mixture was stirred under reflux for 5 h. The reaction vessel was cooled down to room temperature and the reaction mixture was neutralized with saturated sodium bicarbonate solution at 0 °C. Then, the organic solvent was removed at reduced pressure, and the residue dissolved in ethyl acetate, washed with saturated sodium bicarbonate solution, dried over anhydrous sodium sulfate, and concentrated to give methyl 1.39 g 3,4,5-trihydroxybenzoate (7.55 mmol, 86% yield)

as white solid. This compound was used in the next step reaction without further purification.

Potassium carbonate (2.962 g, 21.46 mmol) and 2.5 cm^3 benzyl bromide (20.91 mmol) were added to a solution of 1.321 g methyl 3,4,5-trihydroxybenzoate (7.18 mmol) in 10 cm^3 DMF. The reaction mixture was stirred at 80 °C for 6 h and concentrated at reduced pressure, and the resulting residue was partitioned between water and ethyl acetate. The aqueous layer was extracted further with ethyl acetate and the combined organic layers were dried (Na_2SO_4) and concentrated under reduced pressure. Methyl 3,4,5-tris(benzyloxy)benzoate was obtained as white solid (2.766 g, 6.09 mmol, 85% yield).

A mixture of methyl 2.114 g 3,4,5-tris(benzyloxy)benzoate (4.66 mmol), sodium hydroxide (96 mmol), 6 cm^3 MeOH, and 12 cm^3 dioxane was heated at reflux for 4 h. The solvent was removed and the resulting residue was partitioned between water and ethyl acetate. The combined organic layers were washed with brine, dried (Na_2SO_4), and concentrated at reduced pressure to give the title compound (1.984 g, 4.51 mmol, 97% yield) as a white solid. Spectral data were in accordance with those previously reported [42].

1,2-Bis[[3,4,5-tris(benzyloxy)benzoyl]oxy]benzene (3b) A suspension of 0.971 g 3,4,5-tris(benzyloxy)benzoic acid (2.207 mmol), 0.640 g DCC (3.102 mmol), and 0.122 g DMAP (1.00 mmol) in 40 cm^3 CH_2Cl_2 was stirred, under an argon atmosphere, at 0 °C for 15 min. Then, a solution of 0.110 g 1,2-dihydroxybenzene (1.00 mmol) in 5 cm^3 CH_2Cl_2 was added dropwise, and the reaction was allowed to reach room temperature and stirred overnight. The resulting mixture was filtered through Celite pad and the filtrate partitioned between water and CH_2Cl_2. The combined organic layers were washed with brine, dried (Na_2SO_4), and concentrated at reduced pressure. The crude product was purified by column chromatography ($CHCl_3$–hexane–IPA, 99:0.5:0.5) to give the title compound (0.554 g, 58% yield) as a white solid. Spectral data were in accordance with those previously reported [43].

1,2-Bis[(3,4,5-trihydroxybenzoyl)oxy]benzene (3) A mixture of 0.340 g 1,2-bis[[3,4,5-tris(benzyloxy)benzoyl]oxy]benzene (0.356 mmol) and 10% Pd–C (53.7 mg) in 15 cm^3 EtOAc was stirred at room temperature for 20 h under H_2 atmosphere at 6 atm. The mixture was filtered through a Celite pad and concentrated in vacuo to give the title product as a white solid (0.140 g, 0.338 mmol, 94% yield). Spectral data were in accordance with those previously reported [43].

Enzyme inhibition assays

Catalytic domains of MMP-2, MMP-8, MMP-9, and the fluorogenic substrate (OmniMMP®=Mca-Pro-Leu-Gly-Leu-Dpa-Ala-Arg-NH_2) were purchased from Enzo Life Sciences. The assays were performed in triplicate in 96-well white microtiter plates (Corning, NBS). Inhibitor stock solutions (DMSO, 100 mM) were diluted to seven different concentrations (1 μM–1 mM) in fluorometric assay buffer (50 mM Tris·HCl pH 7.5, 200 mM NaCl, 1 mM $CaCl_2$, 1 μM $ZnCl_2$, and 1% DMSO). Enzyme and inhibitor solutions were pre-incubated in the assay buffer for 15 min at room temperature before the addition of the fluorogenic substrate solution (2.5 μM as final concentration). After further incubation for 2–4 h at 37 °C, fluorescence was measured (λ_{ex} = 340 nm, λ_{em} = 405 nm) using a Perkin-Elmer Victor V3 plate reader. The MMP inhibition activity was expressed as percent inhibition respect control wells that lacked inhibitor. IC_{50} values were calculated from the resultant dose–response curves using GraphPad Prism, and are expressed as mean ± SEM of at least three independent measurements in triplicate.

Acknowledgements The authors thank Ava Yuan Xue for the critical reading of the manuscript.

References

1. Ohigashi H, Murakami A (2004) BioFactors 22:49
2. Mayne ST, Playdon MC, Rock CL (2016) Nat Rev Clin Oncol 13:504
3. Ravindran J, Prasad S, Aggarwal BB (2009) AAPS J 11:495
4. Gupta SC, Kismali G, Aggarwal BB (2013) BioFactors 39:2
5. Nasri H, Baradaran A, Shirzad H, Rafieian-Kopaei M (2014) Int J Prev Med 5:1487
6. Dai SX, Li WX, Han FF, Guo YC, Zheng JJ, Liu JQ, Wang Q, Gao YD, Li GH, Huang JF (2016) Sci Rep 6:25462
7. Solomonov I, Zehorai E, Talmi-Frank D, Wolf SG, Shainskaya A, Zhuravlev A, Kartvelishvily E, Visse R, Levin Y, Kampf N, Jaitin DA, David E, Amit I, Nagase H, Sagi I (2016) Proc Natl Acad Sci USA 113:10884
8. Liotta LA, Tryggvason K, Garbisa S, Hart I, Foltz CM, Shafie S (1980) Nature 284:67
9. Martin MD, Matrisian LM (2007) Cancer Metastasis Rev 26:717
10. Balbin M, Fueyo A, Tester AM, Pendas AM, Pitiot AS, Astudillo A, Overall CM, Shapiro SD, Lopez-Otin C (2003) Nat Genet 35:252
11. Dufour A, Overall CM (2013) Trends Pharmacol Sci 34:233
12. Levy DE, Lapierre F, Liang W, Ye W, Lange CW, Li X, Grobelny D, Casabonne M, Tyrrell D, Holme K, Nadzan A, Galardy RE (1998) J Med Chem 41:199
13. Drummond AH, Beckett P, Brown PD, Bone EA, Davidson AH, Galloway WA, Gearing AJ, Huxley P, Laber D, McCourt M, Whittaker M, Wood LM, Wright A (1999) Ann N Y Acad Sci 878:228
14. Agrawal A, Romero-Perez D, Jacobsen JA, Villarreal FJ, Cohen SM (2008) ChemMedChem 3:812

15. Rubino MT, Maggi D, Laghezza A, Loiodice F, Tortorella P (2011) Arch Pharm (Weinheim, Ger) 344:557
16. Giustiniano M, Tortorella P, Agamennone M, Di Pizio A, Rossello A, Nuti E, Gomez-Monterrey I, Novellino E, Campiglia P, Vernieri E, Sala M, Bertamino A, Carotenuto A (2013) J Amino Acids 2013:178381
17. Di Pizio A, Agamennone M, Aschi M (2012) PLoS ONE 7:e47774
18. Di Pizio A, Agamennone M, Tortorella P (2016) Curr Top Med Chem 16:449
19. Di Pizio A, Laghezza A, Tortorella P, Agamennone M (2013) ChemMedChem 8:1475
20. Thomas NV, Kim SK (2010) Biochem Res Int 2010:845975
21. Smolarz HD, Załuski D (2009) Annales UMCS. Pharmacia 22:89
22. Mahmood T, Akhtar N (2013) Rejuvenation Res 16:91
23. Jha S, Kanaujia SP, Limaye AM (2016) Gene 593:126
24. Fassina G, Vene R, Morini M, Minghelli S, Benelli R, Noonan DM, Albini A (2004) Clin Cancer Res 10:4865
25. Chowdhury A, Nandy SK, Sarkar J, Chakraborti T, Chakraborti S (2017) Mol Cell Biochem 427:111
26. Dell'Agli M, Bellosta S, Rizzi L, Galli G, Canavesi M, Rota F, Parente R, Bosisio E, Romeo S (2005) Cell Mol Life Sci 62:2896
27. Tauro M, Laghezza A, Loiodice F, Piemontese L, Caradonna A, Capelli D, Montanari R, Pochetti G, Di Pizio A, Agamennone M, Campestre C, Tortorella P (2016) J Enzyme Inhib Med Chem 31(sup 4):25
28. Johnson AR, Pavlovsky AG, Ortwine DF, Prior F, Man CF, Bornemeier DA, Banotai CA, Mueller WT, McConnell P, Yan C, Baragi V, Lesch C, Roark WH, Wilson M, Datta K, Guzman R, Han HK, Dyer RD (2007) J Biol Chem 282:27781
29. Ball P (2008) Chem Rev 108:74
30. Ball P (2017) Proc Natl Acad Sci USA 114:13327
31. Southall NT, Dill KA, Haymet ADJ (2002) J Phys Chem B 106:521
32. Michel J, Tirado-Rives J, Jorgensen WL (2009) J Am Chem Soc 131:15403
33. Krimmer SG, Cramer J, Betz M, Fridh V, Karlsson R, Heine A, Klebe G (2016) J Med Chem 59:10530
34. Lin EJ, Zhang X, Wang DY, Hong SZ, Li LY (2014) Bangl J Pharmacol 9:419
35. Ma CY, Ji WT, Chueh FS, Yang JS, Chen PY, Yu CC, Chung JG (2011) J Agr Food Chem 59:9032
36. Decaneto E, Vasilevskaya T, Kutin Y, Ogata H, Grossman M, Sagi I, Havenith M, Lubitz W, Thiel W, Cox N (2017) Phys Chem Chem Phys 19:30316
37. Bertini I, Calderone V, Fragai M, Luchinat C, Maletta M, Yeo KJ (2006) Angew Chem Int Edit 45:7952
38. Grossman M, Born B, Heyden M, Tworowski D, Fields GB, Sagi I, Havenith M (2011) Nat Struct Mol Biol 18:1102
39. Bucher D, Stouten P, Triballeau N (2018) J Chem Inf Model 58:692
40. Dhanaraj V, Williams MG, Ye QZ, Molina F, Johnson LL, Ortwine DF, Pavlovsky A, Rubin JR, Skeean RW, White AD, Humblet C, Hupe DJ, Blundell TL (1999) Croat Chem Acta 72:575
41. Rowsell S, Hawtin P, Minshull CA, Jepson H, Brockbank SM, Barratt DG, Slater AM, McPheat WL, Waterson D, Henney AM, Pauptit RA (2002) J Mol Biol 319:173
42. Nale SD, Jadhav VH (2016) Tetrahedron Lett 57:2652
43. Puig T, Turrado C, Benhamu B, Aguilar H, Relat J, Ortega-Gutierrez S, Casals G, Marrero PF, Urruticoechea A, Haro D, Lopez-Rodriguez ML, Colomer R (2009) Clin Cancer Res 15:7608